

# Distinct abundance patterns in multiple damped Ly $\alpha$ galaxies: Evidence for truncated star formation?<sup>★</sup>

S. Lopez<sup>1</sup> and S. L. Ellison<sup>2,3</sup>

<sup>1</sup> Departamento de Astronomía, Universidad de Chile, Casilla 36-D, Santiago, Chile

<sup>2</sup> European Southern Observatory, Casilla 19001, Santiago 19, Chile

<sup>3</sup> Pontificia Universidad Católica de Chile, Casilla 306, Santiago 22, Chile  
e-mail: sellison@astro.puc.cl

Received 8 August 2002 / Accepted 17 March 2003

**Abstract.** Following our previous work on metal abundances of a double damped Ly $\alpha$  system with a line-of-sight separation  $\sim 2000 \text{ km s}^{-1}$  (Ellison & Lopez 2001), we present VLT UVES abundances of 3 new systems spanning a total of  $\sim 6000 \text{ km s}^{-1}$  at  $z \sim 2.5$  toward the southern QSO CTQ247. These abundances are supplemented with echelle observations of another “double” damped Ly $\alpha$  system in the literature. We propose a definition in terms of velocity shift of the sub-class “multiple damped Ly $\alpha$  system”, which is motivated by its possible connection with large-scale structure. We find that the abundance ratio [S/Fe] is systematically low in multiple systems compared with single systems, and with a small scatter. The same behavior is found in 2 more single DLA systems taken from the literature that show evidence of belonging to a galaxy group. Although [Si/Fe] ratios are also generally lower in multiple DLAs than in single DLAs, the effect is less striking since the scatter is larger and there are a number of low [Si/Fe] DLAs in the literature. We suggest that this can be explained with a combination of detection bias and, to a lesser extent, the scatter in ionization corrections for different absorbers. We investigate whether consistently low  $\alpha/\text{Fe}$  ratios could be due to dust depletion or ionization corrections and find that the former effect would emphasize the observed trend of low  $\alpha/\text{Fe}$  in multiple systems even further. Ionization may have a minor effect in some cases, but at a level that would not change our conclusions. We thus conclude that the low  $\alpha/\text{Fe}$  ratios in multiple DLAs have a nucleosynthetic origin and suggest that they could be explained by reduced star formation in multiple damped Ly $\alpha$  systems, possibly due to environmental effects. There seems to be independent evidence for this scenario from the mild odd-even effect and from the relatively high N/ $\alpha$  ratios we observe in these multiple systems.

**Key words.** quasars: general – quasars: absorption lines – quasars: individual: CTQ247 – galaxies: evolution – galaxies: clusters: general

## 1. Introduction

Damped Lyman Alpha systems (DLAs) in the spectra of high-redshift quasars have promised to be a powerful probe of early metal enrichment in young galaxies. However, despite the considerable effort invested to develop this technique, its full potential has yet to be realized. Although extensive observing campaigns at intermediate resolution have swollen the list of known DLAs (Ellison et al. 2001b; Lopez et al. 2001 and Peroux et al. 2001 are some of the most recent DLA surveys), only a fraction have been followed-up at high resolution to study their chemical properties, investigate dust content, photoionization and metallicity evolution. With the present sample of some 60 abundance measurements some broad trends have been identified (e.g., Prochaska & Wolfe 2002), but the

global picture of star formation (SF) history deduced from these patterns of elemental abundances – likely affected by dust depletion patterns (Hou et al. 2001) – is still unclear. In particular, extracting coherent scenarios of SF histories in individual DLAs, or subsets of absorbers remains a challenging prospect with current data.

One of the great advantages of studying high redshift galaxies in *absorption* is the lack of selection bias associated with cosmological dimming: galaxies are selected based only on gas cross section, irrespective of their intrinsic luminosity. However, this feature may turn out to be a double-edged sword in that extracting coherent chemical enrichment patterns is almost certainly hindered by the mixed morphological representation. Undoubtedly, some of the scatter in relative abundances comes from variable dust depletion, although system-to-system differences persist even after correcting for grain fraction (Vladilo 2002). In order to compare elemental trends in DLAs in a similar manner to, for example,

Send offprint requests to: S. Lopez, e-mail: slopez@das.uchile.cl

<sup>★</sup> The work presented here is based on data obtained at the ESO Very Large Telescopes, programs 68.A-0361(A) and 66.A-0660(A).

**Table 1.** VLT observations of CTQ 247.

Mode	Wavelength [nm]	Exp. Time [s]	Observing Date
FORS2 (GRISM 600B)	345–590	600	Dec. 18 2000
FORS2 (GRISM 600R)	525–745	400	Dec. 18 2000
UVES Dichroic (390+580)	328–445, 476–684	13 500	Oct. 10, 11 and Nov. 17, 2001
UVES Dichroic (437+860)	376–500, 667–1040	10 800	Nov. 17 2001

local stellar abundance studies, a significant refinement in our approach is required. Such a refinement might include isolating particular subsets of DLAs based either on their morphology or some other observed property (e.g. spin temperature; Chengalur & Kanekar 2000).

In this paper, we investigate whether a distinct enrichment trend exists for absorption line systems with close companions in velocity space, which we will refer to as “Multiple Damped Lyman Alpha systems”, or MDLAs.

## 2. The Sub-class “MDLA”

Lopez et al. (2001) identified the existence of three damped Ly $\alpha$  absorbers spanning a total of  $v = 5900 \text{ km s}^{-1}$  at  $z \sim 2.5$  toward the southern quasar CTQ 247, the first ever example of a triple DLA; Ellison et al. (2001b) discovered a double absorption systems for which  $v = 1800 \text{ km s}^{-1}$  at  $z \sim 2$  toward Q2314–409; a similar velocity span as in CTQ 247 is covered by the two DLAs toward Q2359–02 at  $z \sim 2$  (Wolfe et al. 1986). Statistically, these are extremely improbable events if the proximity of the systems is purely by chance, and only these few cases are reported in the literature. It is therefore feasible to postulate that in these cases the multiple absorption systems may be in some way related, rather than chance alignments. However, such large velocities are difficult to reconcile with today’s galaxy groups and clusters – i.e., virialized entities – or even with superclusters. However, at  $z > 0$  current work on small angular fields shows evidence for very large structures on comoving scales as large as  $d \sim 100 h_{100}^{-1} \text{ Mpc}$  ( $\Delta v \sim 10\,000 \text{ km s}^{-1}$  if purely due to Hubble flow) at various redshifts. Evidence for large structure on many Mpc scales has been found in absorbing gas both across (e.g., Williger et al. 2002;  $d \sim 100 h^{-1} \text{ Mpc}$  at  $z \sim 1.3$ ) and along the line of sight (Quashnock et al. 1996;  $d \sim 100 h^{-1} \text{ Mpc}$  at  $z \sim 3$ ), in super-clusters ( $d \sim 20 h^{-1} \text{ Mpc}$  at  $z \sim 0.8$ ; Haines et al. 2003) and in Lyman-break galaxies (Steidel et al. 1998;  $d \sim 10 h^{-1} \text{ Mpc}$  at  $z \sim 3$ ). Large structure has also been reproduced in CDM N-body simulations ( $d \sim 20 h^{-1} \text{ Mpc}$  at  $z \sim 1$ ; Evrard et al. 2002). It therefore seems a feasible (but not exclusive) possibility that absorption systems separated by several thousand  $\text{km s}^{-1}$  may be associated with very large scale structure.

Motivated both by the uniqueness of MDLAs and the possibility of large-structure, we have embarked on a program to measure abundances in these systems. We will define an MDLA as 2 or more DLAs spanning a velocity range

$$500 < \Delta v < 10\,000 \text{ km s}^{-1}. \quad (1)$$

While the upper limit is set to match the limits of the largest structures known at high redshift, the lower velocity roughly corresponds to the largest asymptotic velocities in massive spirals (e.g. Rigopoulou et al. 2002)<sup>1</sup>. Note that this is a *working* definition only; although it might be possible that MDLAs probe some kind of large structure (but see Sect. 5), our definition does not necessarily imply that they host the strong C IV absorption used by Quashnock, vanden Berk & York (1996) or they are associated with the LBGs identified by Steidel et al. (1996).

From an instrumental point of view, identifying MDLAs in Ly $\alpha$  – in contrast to using metal lines – will certainly limit the identification of systems separated by  $\Delta v \lesssim 1000 \text{ km s}^{-1}$ . If the discovery spectrum has poor  $S/N$ , obtaining line parameters for close MDLAs will require both the detection of metal lines, and a good continuum estimation<sup>2</sup>.

For  $N(\text{H I})$  criterion, we will relax the canonical limit to include systems with  $N(\text{H I}) > 10^{20} \text{ cm}^{-2}$ . Not only do systems down to this limit continue to exhibit clear damping wings, but in the following we show that in such range ionization does not yet play a significant role when deriving abundances from low-ions.

The first in-depth study of an MDLA was presented by Ellison & Lopez (2001; hereafter Paper I). There, the two DLAs toward Q2314–409 were noted to have low  $[\text{S}/\text{Fe}]$  ratios, a result which we suggested was due to the possible impact of environment on the chemical abundances in DLA protogalaxies. In the present work, we extend the study of abundances in MDLAs by investigating the triple DLA toward CTQ247 with new echelle data, and including literature abundances of the double system toward Q2359–02. These new abundances reinforce our previous suggestion of peculiar relative abundances in MDLAs.

After presenting the new data in Sect. 3, the discussion of the abundances is given in Sect. 4, where we attempt a statistical comparison between the 2 populations, and assess possible systematic effects that may bias our result. A discussion on the nature of MDLAs is outlined in Sect. 5.

<sup>1</sup> This lower limit will probably exclude the majority of bound galaxy satellites since most local spirals’ satellites have velocity differences of less than  $300 \text{ km s}^{-1}$ , Zaritsky et al. (1997).

<sup>2</sup> Two  $N(\text{H I}) = 2 \times 10^{20} \text{ cm}^{-2}$  DLAs separated by  $\Delta v = 1\,000 \text{ km s}^{-1}$  will mimic a single system in  $FWHM \sim 5 \text{ \AA}$  data if  $S/N \lesssim 20$ , but for  $\Delta v \sim 500 \text{ km s}^{-1}$  they will do so unless  $S/N \gtrsim 50$ .

### 3. Data analysis

#### 3.1. Observations and data reduction

CTQ 247 was observed in service mode with the UVES instrument at the ESO Kueyen telescope in October and November 2001 under good seeing conditions ( $0.6''$ – $1.0''$ ). With the 390+580 and 437+860 dichroic modes we covered from 328 to 1020 nm with two gaps at 576–583 nm and 852–866 nm. The exposure times were 13 500 s for dichroic 1 and 10 800 s for dichroic 2 (Table 1).

After the usual fashion of bias-subtracting and flat-fielding of the individual CCD frames, the echelle orders were extracted and reduced interactively with the UVES pipeline routines (Ballester et al. 2000). The reference Th-Ar spectra used for wavelength calibration were taken after each science exposure. The wavelength values were converted to vacuum heliocentric values and each order of a given instrumental configuration was binned onto a common linear wavelength scale of  $0.04 \text{ \AA pixel}^{-1}$ . The reduced orders were then added with a weight according to the inverse of the flux variances. Finally, the flux values were normalized by a continuum that was defined using cubic splines over featureless spectral regions. The spectral resolution is  $FWHM \sim 6.7 \text{ km s}^{-1}$ , while the typical signal-to-noise ratio per pixel is  $S/N \sim 35$ – $40$ .

In addition to the UVES data, a lower resolution ( $FWHM \approx 3 \text{ \AA}$ ) spectrum of CTQ 247 was obtained on December 18 2000 using FORS2 at the ESO Kueyen Telescope. This spectrum was used to better define the quasar continuum in the spectral region around the damped Ly $\alpha$  lines.

#### 3.2. Column densities

We used FITLYMAN and VPFIT<sup>3</sup> to fit the line profiles with theoretical Voigt profiles. All fits were unconstrained in redshift, Doppler width and column density, unless otherwise stated. In general, we prefer this approach over the apparent optical depth method (AODM; Savage & Sembach 1991) when velocity components are not resolved as is sometimes the case. In addition, when dealing with transitions that lie in the Ly $\alpha$  forest, such as the S II triplet, fitting provides important information to the extent of possible blending. Despite this, however, we did use the AODM for transitions where the fit failed due to line blending of many components or poor  $S/N$ . We adopted the up-to-date  $f$ -values listed in Prochaska et al. (2001) and the solar abundances by Grevesse & Sauval (1998), with updates for O and N by Holweger (2001). Table 2 lists the column densities and derived abundances of all elements covered by our observations.

The H I column density was determined by fitting 3 components to the damped Ly $\alpha$  and Ly $\beta$  profiles in the FORS2 spectrum. The choice of the low resolution spectrum reduces the uncertainties inherent to determining  $N(\text{H I})$  from echelle data, such as badly defined continuum where the damping wings extend over more than one order. We obtained  $N(\text{H I}) = 10^{21.13}$ ,  $10^{21.09}$ , and  $10^{20.47} \text{ cm}^{-2}$ , for the 3 systems centered at  $z_{\text{abs}} = 2.5505$ ,  $2.5950$  and  $2.6215$ . The theoretical profiles are

superposed on the data in Fig. 1. The internal fit errors were 0.02 dex for all 3 H I measurements but we believe a more realistic error is given by  $\pm 0.1$ , which is shown by the dotted curve in the figure. Although the noisy data around Ly $\beta$  constrains H I only marginally, this error seems quite safe, given the higher  $S/N$  at Ly $\alpha$ .

We next give a short description of the metal line fits in each of the 3 DLAs which we henceforth refer to as CTQ 247A, B and C.

CTQ247A ( $z_{\text{abs}} = 2.5505$ ): For this DLA we have identified nonsaturated transitions of N I, Si II, S II, Cr II, Fe II, and Zn II, all of which show 4 velocity components. More (weaker) components are revealed by stronger transitions, e.g. Fe II  $\lambda 2344$ , but these do not contribute significantly to the total column densities. Therefore, in order to avoid introducing too many parameters at intrinsically weak transitions in relatively noisy parts of the spectrum, we proceeded by fitting 4 components. Figure 2 shows the nonsaturated transitions used and their fits. From an analysis of the weaker components we estimate that the obtained column densities encompass  $\sim 90\%$  of the total column density; exclusion of weaker components will lead to only a  $\sim 0.05$  dex difference at  $\log N = 15 \text{ cm}^{-2}$ . The S II 1260 triplet lines fall on the red wings of the damped Ly $\alpha$  lines; consequently, they were fitted simultaneously with the H I fixed at the values found for the FORS data, hence the sub-unity values of the continuum in Fig. 2. In addition, we determine an AODM measurement for Mn II and an upper limit for P II.

CTQ247B ( $z_{\text{abs}} = 2.5950$ ): This DLA has a relatively simple velocity structure. Although the strongest Si II and Fe II transitions have 5 velocity components, these span only  $\sim 80 \text{ km s}^{-1}$ . As expected for such a high H I, O I is saturated and we consider it no further here. Conversely, N I which is often barely detected exhibits a large equivalent width in this system. In fact, two of the  $\lambda 1134$  triplet transitions are saturated. However, the triplet is relatively unblended, as are two of the S II triplet lines. Figure 3 shows the nonsaturated transitions used and their fits. There is an absorption feature at the expected position of P II  $\lambda 963$  but since we suspect contamination by a Ly $\alpha$  forest line we only provide an upper limit on  $N(\text{P II})$ . As for CTQ247A, we also provide an AODM measurement for Mn II.

CTQ247C ( $z_{\text{abs}} = 2.6215$ ): This is the lowest H I DLA of the triplet. For this DLA the bulk of the low ions are divided into 2 “sub-clumps” of 3 and 2 velocity components separated by  $\sim 120 \text{ km s}^{-1}$ . Figure 4 shows the nonsaturated transitions used and their fits. Since this is the DLA with the lowest H I of the 3, fewer species are detected and limits are not very stringent. For example, for sulphur our  $3\sigma$  detection limit is  $\log N(\text{S II}) < 14.3$ . We have attempted a fit for the N I triplet, but a combination of many weak components and Ly $\alpha$  blending makes this a very uncertain result and we regard it as an upper limit due to possible contamination. On the other hand, the low H I allows us to profile fit 2 O I transitions, for which each

<sup>3</sup> Available at <http://www.ast.cam.ac.uk/~rfc/vpfit.html>

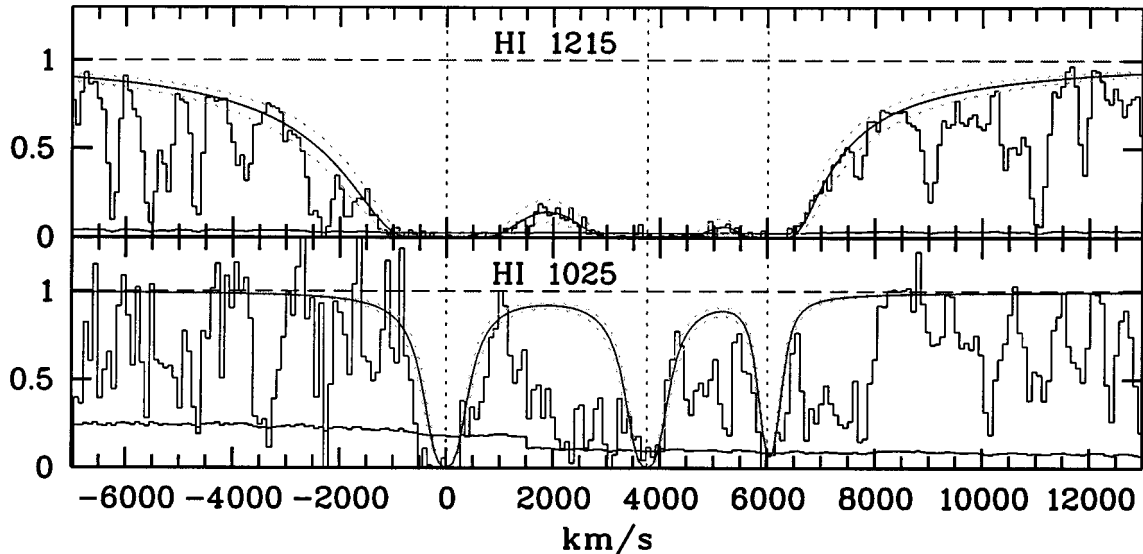


**Fig. 1.** Normalized flux and  $1\sigma$  VLT FORS2 spectrum of CTQ 247 at  $FWHM = 3 \text{ \AA}$  resolution showing the Ly $\alpha$  and Ly $\beta$  lines of the triple DLA. Overlaid is a synthetic Voigt profile of three systems with  $N(\text{HI}) = 10^{21.13}$ ,  $10^{21.09}$ , and  $10^{20.47} \text{ cm}^{-2}$ , centered at  $z_{\text{abs}} = 2.5505$ ,  $2.5950$ , and  $2.6215$ . The dotted lines are  $\pm 0.1$  dex deviations for all  $N(\text{HI})$  values.

one of the 5 components shows at least one nonsaturated line. Also, we report one of the few existing measurements of Al II in DLAs (line positions were held fixed at the Si II values), and one AODM measurement for Al III.

#### 4. Abundances in MDLAs

In Paper I we focused on the relative  $\alpha$  to Fe peak abundances in order to establish whether MDLAs may exhibit distinct SF histories. Similarly, in Fig. 5 the solid circles depict  $[\alpha/\text{Fe}]$  vs.  $[\text{Fe}/\text{H}]$  for the 3 MDLAs presented in this paper (CTQ247A, B, and C), the double DLA Q2314-409A, B (Paper I), and Q2359-02 A, B (Prochaska & Wolfe 1999). The stars are DLAs taken from the literature. Due to the potential problem of blending between S lines and the Ly $\alpha$  forest, we have compiled only values obtained from echelle data. In cases where numbers are present in several references, we have preferred the values by Prochaska et al. (2001) for consistency.

In the following we show statistically that the sub-class MDLA is drawn from a different distribution to single DLAs. We then discuss to which extent dust and ionization effects might produce such a distinction, and what possible systematic effects may be present in the 2 samples.

##### 4.1. Low $\alpha/\text{Fe}$ in MDLAs

As expected in DLAs, all points in Fig. 5 fall over the  $[\alpha/\text{Fe}] = 0$  mark, as both S and Si are  $\alpha$ -chain elements which are created mainly in massive stars on much shorter scales than the long-lived iron producing stars. The ratio of  $[\alpha/\text{Fe}]$  is usually interpreted as an indicator of star formation history and the rate at which the different elements are released into the ISM. In addition to the MDLAs in Fig. 5, we have also plotted DLAs with other neighboring galaxies (usually detected via Lyman break imaging) in the field. These systems are Q0201+112 (Ellison et al. 2001a) which has 4 identified

galaxies in the vicinity, and Q0000-262 (Molaro et al. 2001) for which Steidel et al. (1996) found 2 Lyman break galaxies within  $\Delta z = 0.05$  of the absorber.

The remarkable property to note in Fig. 5 is that all MDLAs systematically show low  $[\text{S}/\text{Fe}]$  values with a small scatter ( $< 0.2$  dex). To quantify this impression, we have performed a modified KS test that provides the likelihood of MDLAs with  $[\text{S}/\text{Fe}]$  measurements to be drawn from a different distribution to single DLAs. We created 1000 realizations of a simulation which recreates the  $[\text{S}/\text{Fe}]$  distribution of literature DLAs and MDLAs including the  $1\sigma$  quoted errors. For each DLA, an error was drawn at random from a Gaussian distribution and added to the observed value<sup>4</sup>. A KS test was then run on each of the 1000 datasets and the likelihood that the KS probability  $P_{\text{KS}}$  was greater than a certain confidence level was calculated from the number of realizations. In this fashion, we overcome 2 problems associated with a normal KS statistics: the small number of MDLAs we have at our disposal and the exclusion of measurement errors.

According to our simulations, the likelihood  $p$  that the two samples are drawn from different distributions is  $p = 1.00$  for  $P_{\text{KS}} > 95\%$  (i.e. every one of the 1000 realizations gives a  $P_{\text{KS}} > 95\%$ ),  $p = 1.00$  for  $P_{\text{KS}} > 98\%$ , and even as high as 0.97 for  $P_{\text{KS}} = 99\%$ . This indicates that the consistently low  $[\text{S}/\text{Fe}]$  values in MDLAs and other multiple systems are statistically significant. Since Si and S are both produced in oxygen burning reactions,  $[\text{S}/\text{Si}] = 0$  in all observed Galactic disk stars (Chen et al. 2002) and we may expect to see similar patterns between S and Si in DLAs. However, the MDLA  $[\text{Si}/\text{Fe}]$  values have a slightly larger dispersion and there are a number of low literature  $[\text{Si}/\text{Fe}]$  values, which renders the two populations less distinguishable. This may be explained because low  $N(\text{S II})$  lines are easily contaminated in the Ly $\alpha$  forest,

<sup>4</sup> We treat the upper limit toward DLA B in Q2314-409 as a detection; a lower value than this does not affect the KS probability.

**Table 2.** Abundance measurements (and  $3\sigma$  upper limits) for CTQ247. <sup>a</sup> uses AODM; <sup>b</sup>  $N(\text{Al}) = N(\text{Al II}) + N(\text{Al III})$ .

X	CTQ247A		CTQ247B		CTQ247C	
	$N(\text{X})$	[X/H]	$N(\text{X})$	[X/H]	$N(\text{X})$	[X/H]
H I	$21.13 \pm 0.10$	...	$21.09 \pm 0.10$	...	$20.47 \pm 0.10$	...
N I	$14.55 \pm 0.03$	$-2.51 \pm 0.10$	$15.07 \pm 0.02$	$-1.95 \pm 0.10$	$< 14.36$	$< -2.04$
O I	...	...	...	...	$15.19 \pm 0.02$	$-2.02 \pm 0.10$
Al II	...	...	...	...	$12.88 \pm 0.07$	$-1.97 \pm 0.12^b$
Al III	$12.81 \pm 0.05^a$	...	$12.63 \pm 0.04^a$	...	$12.33 \pm 0.03^a$	...
Si II	$15.32 \pm 0.04$	$-1.37 \pm 0.11$	$15.59 \pm 0.03$	$-1.06 \pm 0.10$	$13.99 \pm 0.06$	$-2.04 \pm 0.12$
P II	$< 13.15$	$< -1.54$	$< 12.98$	$< -1.67$	...	...
S II	$14.82 \pm 0.06$	$-1.51 \pm 0.12$	$15.19 \pm 0.05$	$-1.10 \pm 0.11$	$< 14.34$	$< -1.33$
Cr II	$13.20 \pm 0.03$	$-1.62 \pm 0.10$	$13.37 \pm 0.04$	$-1.41 \pm 0.11$	...	...
Mn II	$12.86 \pm 0.02^a$	$-1.80 \pm 0.10$	$12.87 \pm 0.01^a$	$-1.75 \pm 0.10$	...	...
Fe II	$14.95 \pm 0.06$	$-1.68 \pm 0.12$	$15.15 \pm 0.02$	$-1.44 \pm 0.10$	$13.60 \pm 0.02$	$-2.37 \pm 0.10$
Fe III	...	...	$< 13.66$	...	...	...
Ni II	$13.94 \pm 0.02$	$-1.44 \pm 0.10$	$13.86 \pm 0.31$	$-1.48 \pm 0.33$	...	...
Zn II	$12.44 \pm 0.05$	$-1.36 \pm 0.11$	$12.68 \pm 0.02$	$-1.08 \pm 0.10$	...	...

whereas low  $N(\text{Si II})$  can be much more easily measured. If we consider only the literature DLAs with Si and S measurements, the KS probability that the two [Si/Fe] samples are consistent is 11%, as opposed to 32% if all are included. There is an obvious outlier in the [Si/Fe] distribution associated with system Q2359–02A; in the following section we argue that this system has anomalously large dust content compared with the rest of the MDLAs and literature DLAs. Discounting this exceptionally dust depleted system reduces the KS probability even further of all [Si/Fe] measurements to 9%. Therefore, although there is a hint that [Si/Fe] may be low in MDLAs, the evidence is not as convincing as that for S. We explore this further in the following section.

#### 4.2. How dust and/or ionization might affect the observed ratios

Before discussing the implications of the observed low  $[\alpha/\text{Fe}]$  ratios in terms of a nucleosynthetic origin, we must first rule out other (non-intrinsic) systematics. In Paper I, we have already discussed the issue of dust and photoionization in the double DLA toward Q2314–409. Here, we embark upon a similar assessment for the CTQ247 triplet. In particular, we investigate whether systematics may cause (a) the  $\alpha/\text{Fe}$  ratio to be lower in MDLAs than in single DLAs; and (b) the  $\alpha$  underabundance in MDLAs to be more evident in S rather than Si.

First, we consider dust depletion. Although disentangling dust depletion from pure nucleosynthetic effects in DLAs is still matter of debate, some broad trends can be established: (1) in no instance is S known to be depleted in the Galactic ISM (e.g. Savage & Sembach 1996). Conversely, Si is mildly depleted in most environments and Fe is very easily incorporated into dust. Therefore, dust depletion will cause an increase in both [S/Fe] and [Si/Fe], the effect being most pronounced in the former ratio, so  $[\text{S}/\text{Si}] > 0$ . (2) Zn is undepleted; thus, assuming the same nucleosynthetic origin as Fe, one expects  $[\text{Zn}/\text{Fe}] > 0$  in dusty systems.

Both in CTQ247A and B the [Zn/Fe] shows a significant departure from solar, indicating that dust is present. This is also true for Q2314–409, the other MDLA for which a Zn abundance is determined; in all cases  $[\text{Zn}/\text{Fe}] > 0.3$ , typical of other DLAs. Therefore, any downward correction due to dust would further emphasize the low  $\alpha/\text{Fe}$  in these MDLAs. It is noteworthy that Q2359–02A, which has the largest [Si/Fe] of all, also shows an unusually large dust content,  $[\text{Zn}/\text{Fe}] = +0.88$ , explaining its anomalously large [Si/Fe]. Not only is Q2359–02A relatively highly depleted compared to other MDLAs, but also in comparison with other DLAs which mostly have  $[\text{Zn}/\text{Fe}] < 0.6$ .

Can low dust content in MDLAs compared with single DLAs be responsible for lower [S,Si/Fe] in the former? Figure 6 shows [S/Si] vs. [S/Fe] for the (few) systems where both elements are available, including 3 MDLAs. It can be seen that apart from one DLA with an extremely large [S/Fe], there is no strong trend for systems with lower [S/Si] (supposedly less dusty) to show lower [S/Fe], suggesting that low S/Fe ratios are not strongly effected by dust. Indeed, the large S abundance measured in Q0307–49 might be due to Ly $\alpha$  blending (Bonifacio et al. 2001) and must be considered with caution. Therefore, low S/Fe is not obviously correlated with low dust content, at least not to the accuracy we can presently measure this ratio. In conclusion, it does not seem from the present sample that a general trend of low  $\alpha/\text{Fe}$  values be driven by any effect of dust, nor do MDLAs have atypical dust content.

We now turn to ionization. Given the large  $N(\text{H I})$  of CTQ247A and B, it is highly unlikely that ionization corrections are required (Viegas 1995). Nonetheless, Prochaska et al. (2002c) found significant corrections in a DLA with  $\log N(\text{H I}) = 20.8$ , so there are occasional cases where photoionization plays a part even in relatively large column density systems. In order to constrain the ionization parameter for CTQ247A and B we use CLOUDY (Ferland 1993) models with a  $\log N(\text{H I}) = 21.1$ , a Haardt-Madau ionizing spectrum (Haardt & Madau 1996) at  $z = 2.3$  and a metallicity of  $10^{-1.5}$  solar, and use the observed ratios to

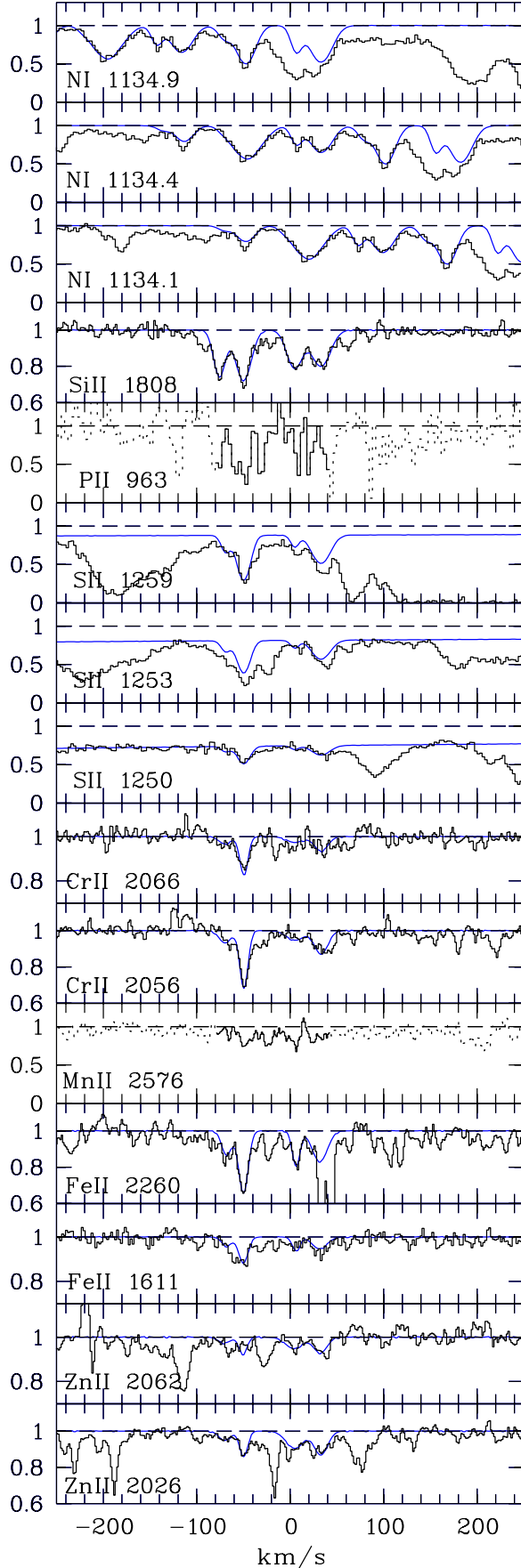


**Fig. 2.** UVES spectrum showing nonsaturated transitions in CTQ247A ( $z_{\text{abs}} = 2.5505$ ). The solid line in the P II and Mn II panels indicates the velocity region used for the AODM.

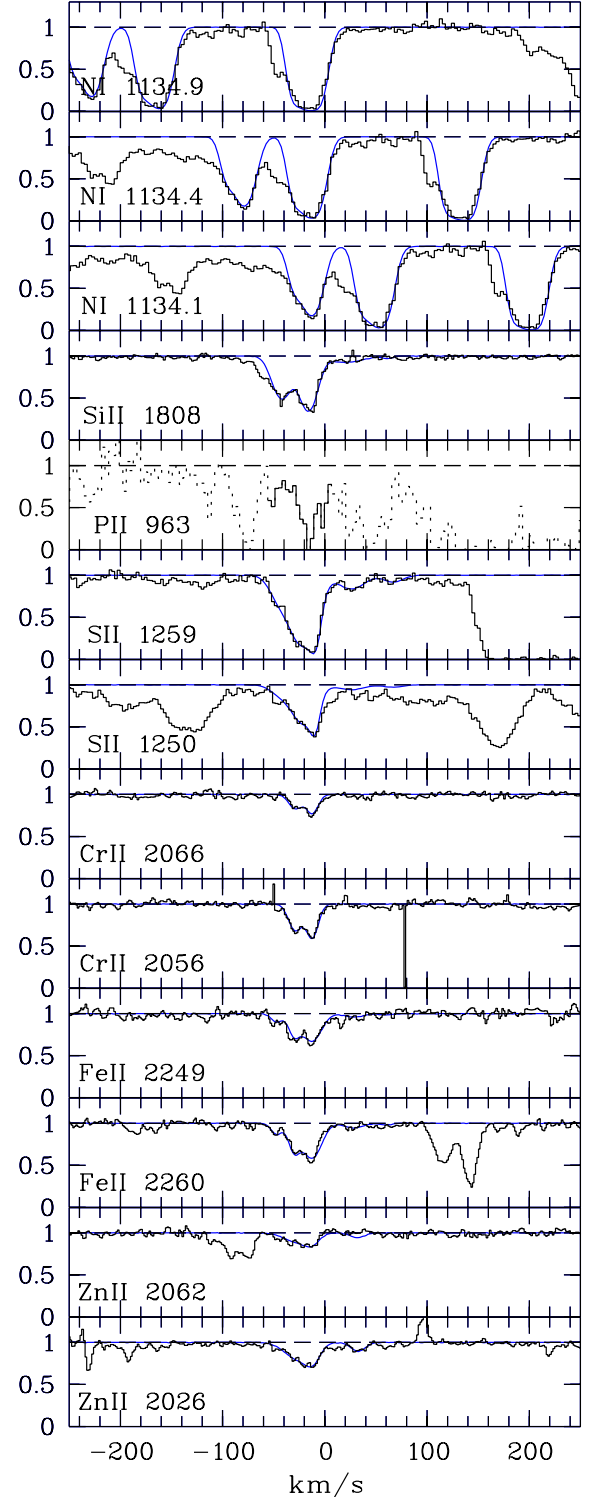


**Fig. 3.** Same as in Fig. 2 but for CTQ247B ( $z_{\text{abs}} = 2.5950$ ).

constrain the ionization parameter. For CTQ247A,  $R \equiv \log N(\text{Al III})/N(\text{Al II})$  provides the most stringent limit on  $\log U$ , whereas the ratio of Fe III/Fe II provides most information on the ionization of CTQ247B. In both cases, the limiting ionization parameter is found to be  $\log U < -3.2$ , see upper panel of Fig. 7. Consequently, this limits the correction to  $[\text{S}/\text{Fe}]$  to be less than 0.07 dex. Note that a correction of this extent is in agreement with the subsolar  $[\text{S}/\text{Si}]$  observed for the

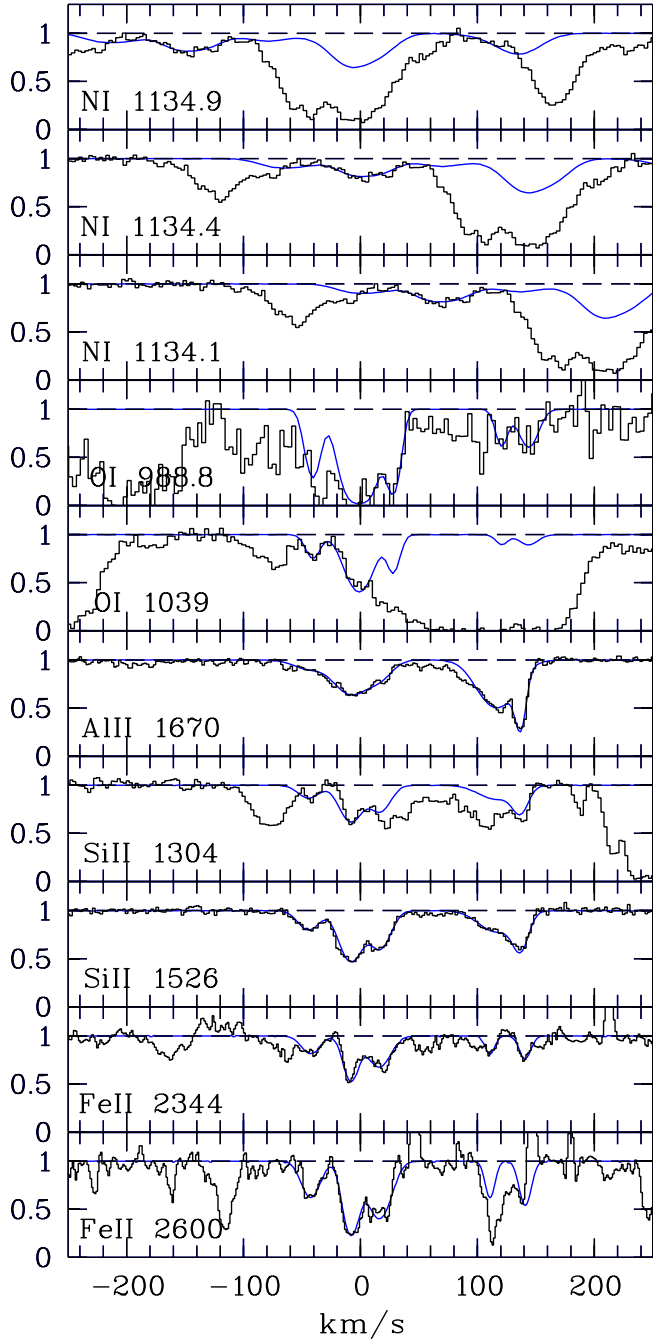


**Fig. 4.** UVES spectrum showing nonsaturated transitions in CTQ247C ( $z_{\text{abs}} = 2.6215$ ).

2 MDLAs in Fig. 6 and brings this ratio into line with solar, within the measurement errors.

CTQ247C has a significantly lower HI column density. Our spectrum does cover the Fe III  $\lambda 1122$  transition but the limit is not very meaningful. However, we can compare Al II and Al III whose ratio has been shown to exhibit a steady trend with  $N(\text{H I})$ , a higher fraction of Al III being present for lower  $N(\text{H I})$  (Vladilo et al. 2001). We find  $R = -0.55$  which is typical of moderate column density DLAs,  $\log N(\text{H I}) > 20.5$ . Repeating the above CLOUDY models with the appropriate HI confirms that the corrections to  $[\text{S}/\text{Fe}]$  will not exceed 0.1 dex in this MDLAs (bottom panel in Fig. 7). Therefore, we would need to

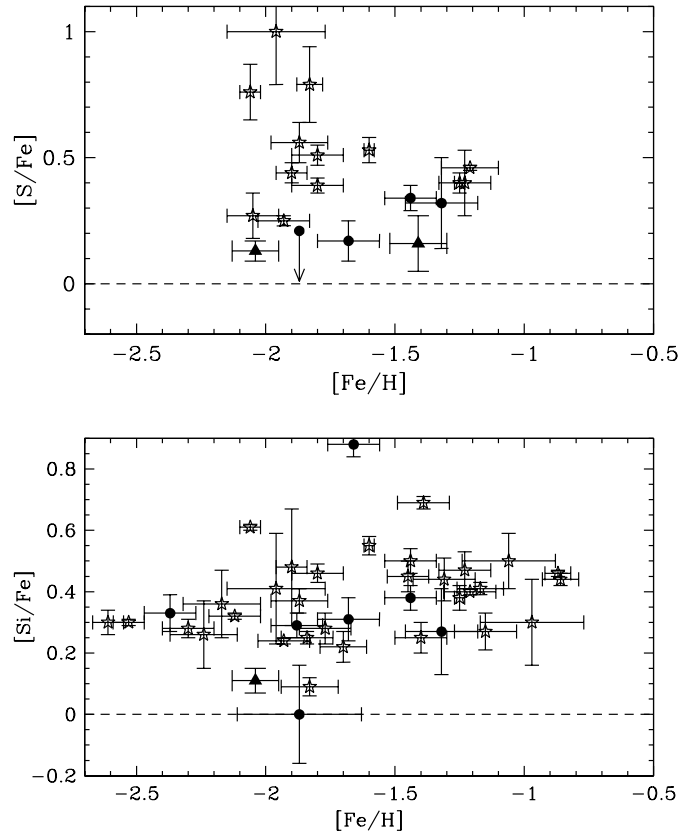


**Fig. 5.** Relative ratios of  $\alpha/\text{Fe}$  for MDLAs (solid circles), the DLAs toward Q0201+1120 and Q0000-262 (solid triangles) and DLAs taken from the literature (stars). All ratios have been corrected to the following solar values:  $\log (\text{S}/\text{H})_{\odot} = -4.80$ ,  $\log (\text{Si}/\text{H})_{\odot} = -4.44$ ,  $\log (\text{Fe}/\text{H})_{\odot} = -4.50$  (Grevesse & Sauval 1998). The data points shown in this plot are listed in Table 3.

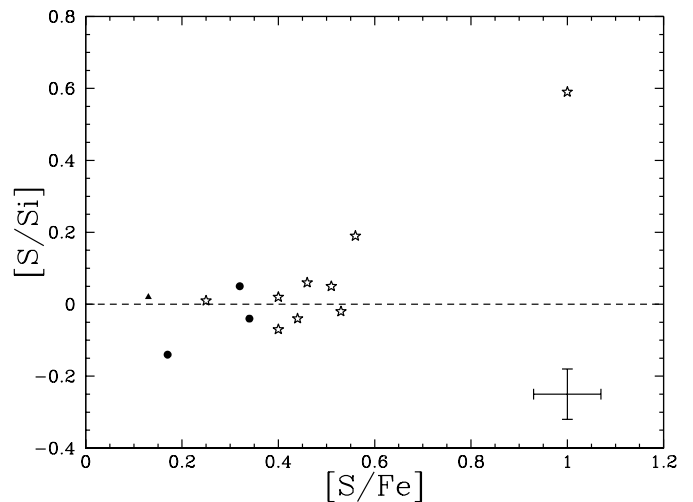


**Fig. 6.**  $[\text{S}/\text{Si}]$  vs.  $[\text{S}/\text{Fe}]$  in MDLAs (circles), single DLAs (stars), and in the DLA toward Q0000-262 (triangle).

make a small upward correction to  $[\text{S}/\text{Fe}]$  of up to about 0.1 dex but this does not alter our conclusions.

We note that the MDLAs toward Q2359-02 both have high  $R \approx -0.3$ , indicating relatively high ionization. According to our CLOUDY models, however, the corrections for  $[\text{S}/\text{Fe}]$

**Table 3.** Abundance ratios: <sup>a</sup>Prochaska et al. (2001); <sup>b</sup>Prochaska & Wolfe (1999); <sup>c</sup>Lu et al. (1998); <sup>d</sup>Lu et al. (1996); <sup>e</sup>Dessauges-Zavadsky et al. (2001); <sup>f</sup>Lopez et al. (1999); <sup>g</sup>Lopez et al. (2002); <sup>h</sup>Bonifacio et al. (2001); <sup>i</sup>Levshakov et al. (2002); <sup>j</sup>Ge et al. (2001); <sup>k</sup>Pettini et al. (2002); <sup>l</sup>Prochaska et al. (2001); <sup>m</sup>Centurion et al. (2000); <sup>n</sup>Prochaska & Wolfe (1996); <sup>o</sup>Dessauges-Zavadsky et al. (in prep.); <sup>p</sup>This paper; <sup>q</sup>Paper I.

QSO	[Fe/H]	[Zn/Fe]	[Si/Fe]	[S/Fe]	Ref.
Q0013–004	–1.83	1.09	...	0.79	m
Q0100+13	–1.90	0.31	0.48	0.44	b,c
Q0149+33	–1.77	0.10	0.28	...	a,b
Q0201+3634	–0.87	0.59	0.46	...	a,n
Q0216+0803A	–0.97	...	0.30	...	d
Q0216+0803B	–1.06	...	0.50	...	d
Q0255+00A	–1.44	...	0.50	...	a
Q0255+00B	–2.05	...	...	0.27	a
Q0307–49	–1.96	...	0.41	1.00	e,h
Q0336–01	–1.80	...	...	0.39	a
Q0347–38	–1.80	–0.10	0.46	0.51	a,h,i
Q0741+474	–1.93	...	0.24	0.25	a
Q0836+11	–1.40	...	0.25	...	a
Q0957+33A	–1.45	...	0.45	...	a
Q0957+33B	–1.87	...	0.37	0.56	a
HE1104–18	–1.60	0.57	0.55	0.53	f
Q1108–07	–2.12	...	0.32	...	a
Q1210+17	–1.15	0.25	0.27	...	a
Q1215+33	–1.70	0.41	0.22	...	a
Q1223+17	–1.84	0.22	0.25	...	a
Q1331+17	–2.06	...	0.61	0.76	a,b,o
Q1409+095A	–2.30	...	0.28	...	k
Q1759+75	–1.21	...	0.40	0.46	a
Q1946+7658	–2.53	...	0.30	...	a
Q2206–19	–0.86	0.45	0.44	...	a
Q2206–19	–2.61	...	0.30	...	a
Q2230+02	–1.17	0.45	0.41	...	a,b
Q2231–00	–1.31	0.54	0.44	...	b
Q2237–060	–2.17	...	0.36	...	c,d
Q2243–603	–1.25	0.13	0.38	0.40	g
Q2343+1232	–1.23	...	0.47	0.40	c,l
Q2344+12	–1.83	...	0.09	...	a
Q2348–01A	–1.39	...	0.69	...	a
Q2348–01B	–2.24	...	0.26	...	a
CTQ247A	–1.68	0.32	0.31	0.17	p
CTQ247B	–1.44	0.36	0.38	0.34	p
CTQ247C	–2.37	...	0.33	<1.04	p
Q2314–409A	–1.32	...	0.27	0.32	q
Q2314–409B	–1.87	...	0.00	<0.21	q
Q2359–02A	–1.66	...	0.88	...	b
Q2359–02A	–1.88	...	0.29	...	b

are still negligible for the corresponding ionization parameter, while [Si/Fe] requires downward corrections of 0.1–0.2 dex.

From a more general point of view, Fig. 7 tells us that for a typical  $\log N(\text{H I}) = 20.5$  DLA the corrections are downward for Si/Fe and upward for S/Fe, whereas at the low end of H I column densities the [Si/Fe] ratio is significantly more sensitive to ionization than [S/Fe] and both corrections are downward (cf. Prochaska et al. 2002c). Ionization will therefore

require downward corrections in [Si/S] but these will not necessarily contribute to the wider spread of MDLA [Si/Fe] values we observe in Fig. 5.

We can quantify the effect of ionization on the comparative dispersion between [Si/Fe] and [S/Fe] by performing Monte-Carlo simulations with a grid of CLOUDY models. To this end, we constructed 2 samples of  $N = 500$  CLOUDY models each, with  $-4 < \log U < -3$  (“low-ionization” sample) and  $-4 < \log U < -2$  (“high+low-ionization” sample), and H I column density and metallicity values uniformly distributed in the ranges  $19.4 < \log N(\text{H I}) < 22.0$ ,  $-2.4 < \log(Z/Z_{\odot}) < -0.8^5$ . To simulate our observations we selected randomly 1 000 sets of 20 DLAs each from the two samples. Their [X/Fe] distributions are shown in the upper panel of Fig. 8. The *difference* between the scatters in [Si/Fe] and [S/Fe] was calculated as  $\Delta S \equiv \sigma[\text{Si/Fe}] - \sigma[\text{S/Fe}]$ , where  $\sigma[\text{X/Fe}]$  is the standard deviation of each dataset. The bottom panel of the figure shows the  $\Delta S$  distribution for both samples. For the low+high-ionization sample the probability  $P(\Delta S > 0)$  of having a wider scatter in [Si/Fe] is roughly 0.7, while  $P(\Delta S > 0) = 0.85$  if the DLAs are drawn exclusively from the low-ionization sample. This is an indication that ionization does affect the distributions differentially, although the differences are generally below measurement errors.

#### 4.3. Other possible systematic effects

Finally, other possible systematic effects we have to beware of are: (1) column densities: our column densities come from  $\chi^2$  fits whereas the majority of literature DLAs have AODM measurements. However, it is well established that both approaches give essentially same results provided the lines are nonsaturated as is our case. (2) Solar abundances: solar abundances have undergone some significant revisions in recent years; all the points in figures 5 and 9 have been put on a common solar scale. (3) Atomic data: some  $f$ -values have changed in recent years, most notably Fe II  $\lambda 1611$ . However, this should not be an issue as long as very few systems rely on only one transition<sup>6</sup>. (4) Blending: S II transitions are normally in the forest and therefore particularly susceptible to contamination. This is especially a worry if the AODM is used since it would cause larger  $N(\text{S})$  if contamination is present. Since 40% of literature S measurements comes from the UCSD database which uses the AODM, in theory we could have compared our data with overestimations of S/Fe. However, checking in Prochaska et al. (2001) on a case-by-case basis shows that this is unlikely to be a problem because the possibility of contamination was carefully assessed in each case. Even excluding [S/Fe] points determined by AODM from Fig. 5 still shows the low S trend in MDLAs. (5) Instrument: almost all literature abundances come from HIRES data whereas we have used UVES at a slightly higher resolution. However, some

<sup>5</sup> Of course, uniformly distributed values of H I and Z do not represent the observed distribution of DLAs, this range is purely for the purpose of investigating the effects of ionization.

<sup>6</sup> e.g., Q2206–19A is the only DLA in the sample that relies solely on Fe II  $\lambda 1611$ .



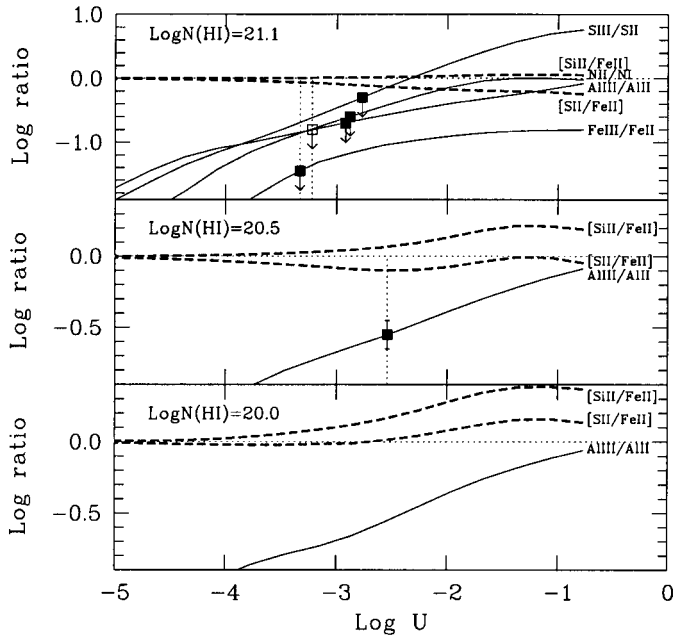


**Fig. 7.** Ratio of doubly to singly ionized species as a function of ionization parameter  $U$  from CLOUDY models with a Haardt & Madau (Haardt & Madau 1996) ionizing spectrum. Top panel: model with  $\log N(\text{H I}) = 21.1$  and gas metallicity  $\log Z = \log Z_{\odot} - 1.5$  compared with data points for CTQ247A (open square) and CTQ247B (filled squares). Middle panel: the measured AlIII/AlII ratio for CTQ247C, and a model using  $\log N(\text{H I}) = 20.5$  and metallicity  $\log Z = \log Z_{\odot} - 2.5$ . Bottom panel: a model using  $\log N(\text{H I}) = 20.0$ , the column density cutoff in our definition of MDLAs, and metallicity  $\log Z = \log Z_{\odot} - 1.5$ . In all panels the dashed lines indicate solar-corrected ratios while the solid lines are for column density ratios.

high  $\alpha/\text{Fe}$  UVES values in Table 3 and the low  $\alpha/\text{Fe}$  HIRES value in the MDLAs toward Q2359–02 show that a possible bias due to different data type is unfounded.

In summary, we have found that MDLAs exhibit significantly lower  $[\text{S}/\text{Fe}]$ , and to a less striking extent,  $[\text{Si}/\text{Fe}]$  ratios than single DLAs taken from the literature. We have argued that these low values are not driven by ionization differences or dust depletion, although an observational bias may be partially responsible for the clearer abundance distinction in S compared to Si. Having excluded the main systematic effects, these results therefore imply a nucleosynthetic origin for differences in abundance ratios between MDLAs and single DLAs.

## 5. Discussion

### 5.1. The nature of MDLAs

If the typically low values of  $[\alpha/\text{Fe}]$  of MDLAs are truly nucleosynthetic in origin, this may indicate that these systems either represent a particular galaxy type or that they share a common evolutionary or environmental link. The first issue to address is whether the “multiplicity” is indeed due to more than one distinct galaxy. Schaye (2001) has suggested that some DLAs may be associated with winds, in which case MDLAs may be caused by outflowing material from the parent DLA. Indeed, Nulsen et al. (1998) have shown that large scale galactic winds

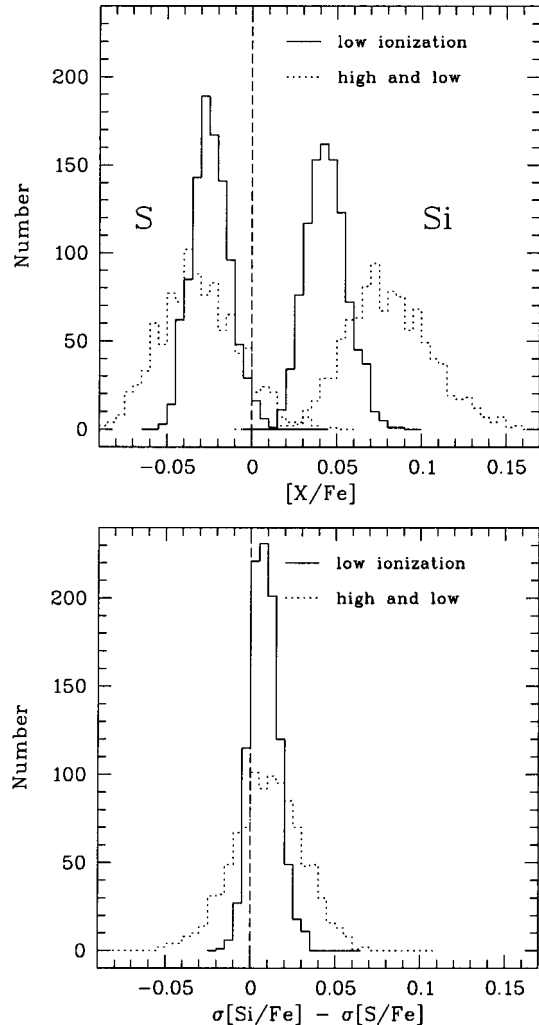


**Fig. 8.** Simulated  $[\text{S}/\text{Fe}]$  and  $[\text{Si}/\text{Fe}]$  distributions (top panel) and difference between their scatters (bottom panel). The solid (dotted) histogram shows DLA simulations drawn from a sample of DLAs with  $-4 < \log U < -3$  ( $-4 < \log U < -2$ ).

can produce column densities equal to those of DLAs. This could be tested by studying abundances in systems that are effectively transverse multiple systems, that is DLAs observed in more than one line of sight separated by many tens of kpc. The closest example we have of this in the current dataset is the case of Q0201+1120 (Ellison et al. 2001a) which is located in a concentration with at least four other galaxies and indeed shows low  $[\text{S}/\text{Fe}]$ , possible evidence that the abundance trend is symptomatic of a group environment rather than simply line of sight velocities within a single object.

However, this evidence remains vague in our context of MDLAs as these imaging studies deal only with DLAs without line-of-sight companions. Deep imaging and subsequent spectroscopy of the fields toward CTQ247 and Q2314–409 as well as control fields around QSOs harboring single DLAs is therefore required in order to pursue a comparison of possibly different environments. At higher redshifts, finding evidence for cluster environments of single DLAs (and even the DLA absorbers themselves) has proven difficult (Gawiser et al. 2001; Prochaska et al. 2002a), so much work is still to be done in

this direction. Similarly, although several DLA imaging studies have been carried out (e.g., Le Brun et al. 1997), we lack studies of the clustering properties in the DLA fields at  $z < 1.0$  and there are currently no known MDLAs at low redshift.

### 5.2. Truncated star formation in MDLAs?

As suggested in Paper I, the low  $\alpha/\text{Fe}$  abundances observed in MDLAs might be due to suppressed SF in the galaxies harboring the absorbing gas. We now raise the question as to whether environment may cause these observed abundance anomalies and speculate upon the possibility that MDLAs arise in “protogalactic groups”.

There is a clear trend of galaxies in rich environments out to  $z \lesssim 0.5$  to exhibit suppressed SF, not just in dense cluster cores, but also in clusters out to 2–3 virial radii (Balogh et al. 1997; Lewis et al. 2002) and perhaps out to several Mpc (Pimbblet et al. 2001). The line diagnostics of these galaxies indicate that radial trends are consistent with an age sequence in which the last episode of star formation happened most recently in the outermost galaxies (Balogh et al. 1999). However, the physical mechanisms governing this effect are not clear; violent processes such as ram pressure stripping (e.g., Couch et al. 2001 and references therein) and passive exhaustion of gas supply (e.g., Balogh et al. 1999) are the two main possibilities. The recent finding by Lewis et al. (2002) that local density is the dominant parameter in suppressing SF rates indicates that extreme cluster-scale processes such as ram-stripping by the ICM play a minor role. These results also point to the possibility that reduction in SF need not take place within the gravitational bounds of existing virialized clusters and may occur already in looser groups before they are accreted onto larger structures. This ties in with cluster histories at lower redshifts, because although Dressler et al. (1999) find a significant post-starburst population in clusters, there is evidence that this fraction is not greater than among the field population (Balogh et al. 1999).

If the same physical processes are on-going at high redshifts, then suppressed SF may be evident in galaxies associated with early proto-clusters, such as those identified by Steidel et al. (1998), even though canonical, virialized clusters have yet to form. Although the abundance ratios for MDLAs that we have discussed here are distinct from “field” DLAs, they have typical metallicities for their redshift (cf. Pettini et al. 1999) and moderate dust content. These properties are indications that some chemical maturity has indeed taken place, and MDLAs are similar to other DLAs in terms of their general enrichment. However, the low  $[\alpha/\text{Fe}]$  is an indication that what sets MDLAs apart is that they have been evolving quiescently, without any further major SF episodes, over the last  $\sim 500$  Myrs.

### 5.3. Other evidence for quiescent star formation

If the low  $\alpha/\text{Fe}$  ratios observed in MDLAs are to be explained by quiescent SF, then we should expect to see its signature in other elemental ratios that also act as “cosmic clocks”. The most promising possibility is the  $N/\alpha$  ratio which traces

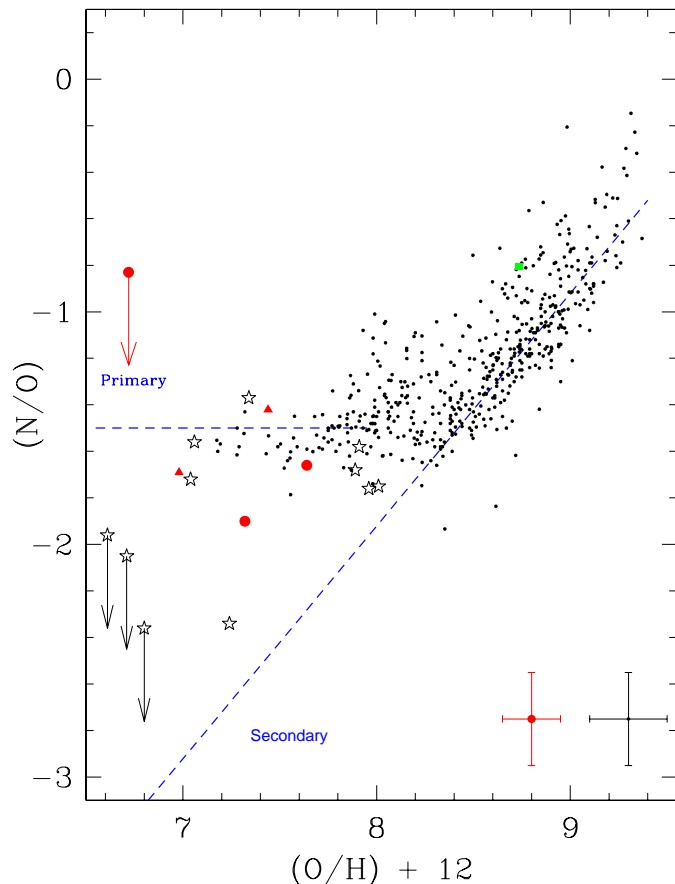


**Fig. 9.** The  $N/\alpha$  ratio in MDLAs (circles), “field” DLAs (stars) and H II regions (dots; see Pettini et al. 2002 for references). The triangles are for the 2 DLAs with companion LBGs.

the primary and secondary contributions from stars of different masses (Henry et al. 2000). Figure 9 shows the  $N/\alpha$  ratio in MDLAs, “field” DLAs and H II regions (Pettini et al. 2002). We only used measurements of O or S in the plot and corrected S values by the solar S/O ratio (1.54 dex). Prochaska et al. (2002b) have suggested a bimodal distribution of  $N/\alpha$  and although this needs to be confirmed by more data, it is clear that a number of DLAs exhibit low ratios. For MDLAs, the ratios are all high, with no points  $(N/O) < -1.9$ , supporting the quiescent SF scenario. It perhaps indicates more chemical maturity than average, but also that the role of massive stars in polluting the ISM of MDLAs may be less important.

The other established trend with metallicity in Galactic stars is the odd-even effect. Although this is not technically a chronometer in the same sense as  $N$  and the alpha elements, there is a correlation with metallicity which may be due to metallicity dependent yields (Goswami & Prantzos 2000). At our disposal we have  $[\text{Mn}/\text{Fe}] = -0.12 \pm 0.08$  (CTQ247A) and  $[\text{Mn}/\text{Fe}] = -0.31 \pm 0.03$  (CTQ247B), the former of which is among the highest values in DLAs of this metallicity (Ledoux et al. 2002; Dessauges-Zavadsky et al. 2002). If these high ratios are not due to dust depletion (Fe is more depleted in the local ISM than Mn) or ionization, they show a mild odd-even effect. Analogously,

$[Al/Si] = 0.07 \pm 0.12$  in CTQ247C, the highest value ever measured, and  $[Al/Si] = -0.28 \pm 0.18$  in B2314–409B (Paper I), which is among the highest values after the  $z = 2.154$  MDLA toward Q2359–02 (Prochaska & Wolfe 2002). Altogether, the odd-even effect seems to be mild in those MDLAs where we can measure it. Since models of massive star yields give good agreement with observations of Mn/Fe in Galactic stars (Goswami & Prantzos 2000; and references therein) and also DLAs (Ledoux et al. 2002), the lack of odd-even effect at low metallicity in MDLAs indicates again that high-mass stars have not been the dominant metal pollutant in MDLAs. This may be interpreted as further evidence that there have not been several epochs of SF building on the enriched interstellar media from previous episodes; further support of suppressed SF.

## 6. Summary

We have studied a sample of 7 DLAs with line-of-sight companions, “multiple” DLAs in our nomenclature, and 2 DLAs arising in transverse groups. We have shown that the relative abundances in these two sub-samples are unusual as compared with single DLAs. In particular, the  $[S/Fe]$  and  $[Si/Fe]$  ratios are statistically lower than literature DLAs, although the effect is more striking in  $[S/Fe]$ . We suggest that this difference is due to (1) an observational bias against measuring low S column densities because weak S II are usually lost in the forest; and (2), to a lesser degree, the larger scatter induced in  $[Si/Fe]$  by photoionization. Besides low  $\alpha/Fe$  ratios, MDLAs also exhibit a mild odd-even effect and relatively high  $N/\alpha$  ratios. We interpret these results as truncated star formation in MDLAs. If the multiplicity of these DLAs is due to grouping in physical space, a thesis we cautiously support, environment may be the cause of the quiescent SF scenario, just as is observed in more nearby clusters and groups of galaxies.

*Acknowledgements.* We are grateful to the anonymous referee for many qualified comments and suggestions on a first version of this paper. We also thank Eric Gawiser for fruitful discussions and comments, Michael Rauch for allowing us to use the FORS data of CTQ247, Max Pettini for providing us with the template for Fig. 9, Mirka Dessauges-Zavadsky for communicating abundances in advance of publication, and Jason Prochaska, whose database at <http://kingpin.ucsd.edu/~hiresdla/> we have consulted. SL acknowledges support from the Chilean *Centro de Astrofísica* FONDAF No. 15010003, and from FONDECYT grant N°3 000 001.

## References

- Ballester, P., Modigliani, A., Boitquin, O., et al. 2000, *ESO Messenger*, 101, 31
- Balogh, M., Morris, S., Yee, H. K. C., Carlberg, R. G., & Ellingson, E. 1999, *ApJ*, 527, 54
- Balogh, M., Morris, S., Yee, H. K. C., Carlberg, R. G., & Ellingson, E. 1997, *ApJ*, 488, L75
- Bonifacio, P., Caffau, E., Centurion, M., Molaro, P., & Vladilo, G. 2001, *MNRAS*, 325, 767
- Centurion, M., Bonifacio, P., Molaro, P., & Vladilo, G. 2000, *ApJ*, 536, 540
- Chen, Y. Q., Nissen, P. E., Zhao, G., & Asplund, M. 2002, *A&A*, 390, 225
- Chengalur, J. N., & Kanekar, N. 2000, *MNRAS*, 318, 303
- Couch, W., Balogh, M., Bower, R., et al. 2001, *ApJ*, 549, 820
- Dessauges-Zavadsky, M., Prochaska, J., & D’Odorico, S. 2002, *A&A*, 391, 801
- Dessauges-Zavadsky, M., D’Odorico, S., McMahon, R. G., et al. 2001, *A&A*, 370, 426
- Dressler, A., Smail, I., Poggianti, B., et al. 1999, *ApJS*, 122, 51
- Ellison, S. L., & Lopez, S. 2001, *A&A*, 380, 117, Paper I
- Ellison, S. L., Pettini, M., Steidel C. C., & Shapley, A. 2001a, *ApJ*, 549, 770
- Ellison, S. L., Yan, L., Hook, I., et al. 2001b, *A&A*, 379, 393
- Evrard, A. E., MacFarland, T. J., Couchman, H. M. P., et al. 2002, *ApJ*, 573, 7
- Ferland, G. J. 1993, University of Kentucky, Physics Department Internal Report
- Gawiser, E., Wolfe, A. M., Prochaska, J. X., et al. 2001, *ApJ*, 562, 628
- Goswami, A., & Prantzos, N. 2000, *A&A*, 359, 191
- Grevesse, N., & Sauval, A. J. 1998, *Space Sci. Rev.*, 85, 161
- Haardt, F., & Madau, P. 1996, *ApJ*, 461, 20
- Haines, C., Campusano, L. E., & Clowes, R. 2002 [[astro-ph/0301473](http://arxiv.org/abs/astro-ph/0301473)]
- Henry, R. B. C., Edmunds, M. G., & Köppen, J. 2000, *ApJ*, 541, 660
- Holweger, H. 2001, in *Solar and Galactic Composition*, ed. R. Wimmer-Schweingruber (Berlin: Springer), 23
- Hou, J. L., Boissier, S., & Prantzos, N. 2001, *A&A*, 370, 23
- Le Brun, V., Bergeron, J., Boisse, P., & Deharveng, J. M. 1997, *A&A*, 321, 733
- Ledoux, C., Bergeron, J., & Petitjean, P. 2002, *A&A*, 385, 802
- Levshakov, S. A., Dessauges-Zavadsky, M., D’Odorico, S., & Molaro, P. 2002, *ApJ*, 565, 696
- Lewis, I., Balogh, M., De Propris, R., et al. 2002, *MNRAS*, 334, 673
- Lopez, S., Reimers, D., Rauch, M., Sargent, W. L. W., & Smette, A. 1999, *ApJ*, 513, 598
- Lopez, S., Maza, J., Masegosa, J., & Marquez, I. 2001, *A&A*, 366, 387
- Lopez, S., Reimers, D., D’Odorico, S., & Prochaska, J. X. 2002, *A&A*, 385, 778
- Lu, L., Sargent, W. L. W., & Barlow, T. A. 1998, *AJ*, 115, 55
- Lu, L., Sargent, W. L. W., Barlow, T. A., Churchill, C. W., & Vogt, S. 1996, *ApJS*, 107, 475
- Molaro, P., Levshakov, S. A., D’Odorico, S., Bonifacio, P., & Centurion, M. 2001, *ApJ*, 549, 90
- Nulsen, P. E. J., Barcons, X., & Fabian, A. C. 1998, *MNRAS*, 301, 168
- Petroux, C., Storrie-Lombardi, L. J., McMahon, R. G., Irwin, M., & Hook, I. M. 2001, *AJ*, 121, 1799
- Pettini, M., Ellison, S. L., Bergeron, J., & Petitjean, P. 2002, *A&A*, 391, 21
- Pettini, M., Ellison, S. L., Steidel, C. C., & Bowen, D. V. 1999, *ApJ*, 510, 576
- Pimbblet, K., Smail, I., Edge, A., et al. 2001, *MNRAS*, 327, 588
- Prochaska, J. X., Gawiser, E., Wolfe, A. M., et al. 2002a, *AJ*, 123, 2206
- Prochaska, J. X., Henry, R., O’Meara, J., et al. 2002b, *ApJ*, accepted
- Prochaska, J. X., Howk, J. C., O’Meara, J. M., et al. 2002c, *ApJ*, 571, 693
- Prochaska, J. X., & Wolfe, A. 2002, *ApJ*, 566, 68

- Prochaska, J. X., Wolfe, A. M., Tytler, D., et al. *ApJS*, 2001, 137, 21
- Prochaska, J. X., Gawiser, E., & Wolfe, A. M. 2001, *ApJ*, 552, 99
- Prochaska, J. X., & Wolfe, A. M. 1999, *ApJS*, 121, 369
- Prochaska, J. X., & Wolfe, A. M. 1996, *ApJ*, 470, 403
- Quashnock, J. M., vanden Berk, D. E., & York, D. G. 1996, *ApJ*, 472, 69
- Rigopoulou, D., Franceschini, A., Aussel, H., et al. 2002, *ApJ*, 580, 789
- Savage, B. D., & Sembach, K. R. 1991, *ApJ*, 379, 245
- Savage, B. D., & Sembach, K. R. 1996, *ARA&A*, 34, 279
- Schaye, J. 2001, *ApJ*, 559, L1
- Steidel, C. C., Adelberger, K. L., Dickinson, M., et al. 1998, *ApJ*, 492, 428
- Steidel, C., Giavalisco, M., Pettini, M., Dickinson, M., & Adelberger, K. 1996, *ApJ*, 462, L17
- Viegas, S. M. 1995, *MNRAS*, 276, 268
- Vladilo, G., Centurión, M., Bonifacio, P., & Howk, J. C. 2001, *ApJ*, 557, 1007
- Vladilo, G. 2002, *ApJ*, 569, 295
- Williger, G. M., Campusano, L. E., Clowes, R. G., & Graham, M. J. 2002, *ApJ*, 578, 708
- Wolfe, A. M., Turnshek, D. A., Smith, H. E., & Cohen, R. D. 1986, *ApJS*, 61, 249
- Zaritsky, D., Smith, R., Frenk, C., & White, S. D. M. 1997, *ApJ*, 478, 39